

Energy- and angular-dependent secondary-electron emission from a silicon (111) 7×7 surface. Emission from bulk states*

P. E. Best

Department of Physics, and The Institute of Materials Science, University of Connecticut, Storrs, Connecticut 06268

(Received 22 October 1975)

Energy- and angular-dependent secondary-electron emission (EADSEE) spectra from a silicon (111) 7×7 reconstructed surface are reported. Only spectra which consist of electrons that have emerged from bulk states are considered here. The spectra are interpreted in terms of the conventional three-step model, in which electrons are excited into high-lying conduction states, move to the surface, and emerge into the vacuum. Microscopic models are considered for the processes that contribute to each of the three steps. The processes which are important in determining the shape of these EADSEE spectra have been identified by comparing the predictions of the models with the observed spectra. The shape of the EADSEE spectra between 6 and 40 eV is determined mostly by the incoherent scattering that occurs as the electrons cross the reconstructed layer. This scattering obliterates the structure in the internal hot-electron distribution, structure which is observed in the spectra of electrons which emerge from a (111) 1×1 unreconstructed surface. For emergence energies below 6 eV there is evidence for a number of processes. It is found that the spectral shape of the internal flux is dominated by structure in the density of conduction states, as first described by Kane. This shape is modified somewhat by energy-dependent transport losses. Most of the observed low-energy (< 6 eV) electrons have emerged coherently through the surface. The energy and angular structure in the low-energy secondary flux is affected in a number of ways in this emergence process. Evidence is seen for diffraction, refraction, and reflection of the emerging electrons. Diffraction at the surface causes peaks in the internal electron distribution to appear at angles of emergence not otherwise expected. Refraction of the outgoing waves leads to a cosine dependence of the angular plot of the secondary current for fixed energies. Reflection of the outgoing electrons at the surface barrier causes a decrease in the number of secondaries. With certain assumptions the reflection (transmission) coefficient of electrons at the barrier, and the wave-vector dependence of this coefficient, can be deduced from the data.

I. INTRODUCTION

The energy and angular dependence of secondary-electron emission (EADSEE)¹ from a silicon (111) 7×7 surface are reported and discussed in these two papers.² The angle-resolved energy spectra of the secondary current, $j_s(E, \Omega_0)$, are measured for each of a series of emergent angles Ω_0 . The same information can also be displayed as $j_s(E_0, \Omega)$ curves which are known as angular plots. The most commonly measured angular plot is of current versus the polar angle θ , $j_s(E_0, \theta)$, for one value of azimuthal angle.

Since 1902 secondary-electron emission (SEE) has been studied for both scientific and technical reasons.³ From the scientific point of view the maximum activity in the subject preceded the 1960s, a period in which a number of review articles appeared.^{4,5} The achievements of that period are perhaps best represented by the successes of the semiempirical models that describe several properties of observed yield curves and energy spectra. Interpretations used then, as now, are based on a three-step model in which electrons are excited into high-lying conduction states, move to the surface, often with intermediate scattering, and finally emerge into the vacuum. De-

tailed theoretical studies have given justification for a similar three-step model used in the interpretation of photoemission data.⁶

There have been few previous studies of EADSEE from single crystals, as the technology to carry out these measurements conveniently has become available only recently. The first study was made on nickel by Jonker⁷ who recorded $j_s(E_0, \theta)$ for secondary energies ranging from 1.5 to 100 eV. At each E_0 the secondary current varied as the cosine of the angle between the surface normal and the direction of emergence. Jonker concluded that the externally observed cosine distribution implied an internal distribution of the same angular dependence. This view is not consistent with currently accepted models of secondary-electron emission, as described below. The nickel surface was cleaned by flashing at 1000°C, a technique that is known now to produce an ordered surface layer which contains carbon.⁸

Burns studied EADSEE from carefully prepared (100) faces of copper and nickel.⁹ With angular and energy resolutions of 4° and 10 eV, respectively, he detected an angular dependence that differed markedly from the previously observed cosine behavior. Features in the $j_s(E_0, \Omega)$ curves were attributed to band-structure effects, although

Burns recognized that more detailed experiments were needed before EADSEE studies could contribute to our knowledge of the electronic structure of metals.

Appelt measured EADSEE from a (110) face of copper, with angular and energy resolutions of 4° and 5 eV, respectively.¹ He saw considerable structure in the $j_s(E_0, \theta)$ curves. Like Burns, Appelt associated EADSEE structure with bulk electronic band structure. Their analyses were criticized by Seah who pointed out that they used a free-electron model to deduce non-free-electron band structures.¹⁰

EADSEE from a silver (111) surface was measured by Seah, with angular and energy resolutions of 6° and 0.2 eV, respectively.¹¹ Two peaks were observed in the energy spectrum of electrons emerging along the surface normal. Seah observed that the peaks exhibited an angular dependence that could not be explained in terms of a nearly-free-electron model for emission from bulk states. He therefore tentatively associated the features with a surface excitation. However, the calculated band structure and density-of-states curve he used show gross departures from nearly-free-electron behavior. In this case there is no reason to expect the EADSEE to reflect nearly-free-electron behavior, and it is therefore concluded that the origin of the observed features has not been identified.

Measurements of EADSEE by Koshikawa *et al.* were made primarily to elucidate processes of importance in the performance of scanning electron microscopes.¹² They observed $j_s(E, \Omega_0)$ curves that varied smoothly with energy and $j_s(E_0, \theta)$ curves which display the cosine behavior that had been observed by Jonker. The surface of the iron single crystal that was studied contained sulfur and gave rise to a $c \ 2 \times 2$ elastic low-energy-electron diffraction (ELEED) pattern.

Structure in EADSEE from a silicon (111) 7×7 surface has been interpreted in terms of emission from surface-state resonances.¹³ To describe this emission a two-step model was used: Electrons are excited into surface-state resonances which lie above the vacuum level, and then emerge into the vacuum. Structure interpreted in this manner was not observed in spectra from the unreconstructed surface and could not be interpreted in terms of models for emission from bulk states. Observations relating to these measurements will be discussed in another paper.² The structure observed in the spectra reported here cannot be interpreted in these terms. The processes to be considered in this paper include only those in which the observed secondaries result from an excitation originally within the bulk of the solid.

Two facts emerge from these few observations. In the experiments of Jonker and of Koshikawa *et al.*, in which cosine behavior of $j_s(E_0, \theta)$ was observed, the bulk crystal structure did not extend completely to the vacuum but was covered by an ordered layer which contained impurity atoms. In the case where an ELEED pattern characteristic of the unreconstructed surface is observed, or where the cleaning procedures used are known to produce an unreconstructed surface, considerable structure is observed in EADSEE. Attempts have been made to relate this structure to the bulk electronic structure of the crystal studied.

The first goal of the present work is to understand the two main observations of the earlier experimental investigations. It is believed that the relationship between structure in EADSEE and the bulk band structure has been correctly described in a model first presented by Kane¹⁴ and supported by the experimental work of Willis and others.^{15,16} In this model, which will be described in detail later, density-of-conduction-states structure is prominent in the energy distribution of the hot electrons. If the majority of these excited electrons emerge into the vacuum without inelastic scattering the density-of-states structure would be a prime cause of structure in the EADSEE data.

From the earlier EADSEE measurements it was pointed out that cosine behavior in $j_s(E_0, \theta)$ curves was observed for reconstructed surfaces that contained impurities. This observation gives rise to the suggestion that scattering of the beam as it emerges through the reconstructed or impurity layer is responsible for the cosine behavior. This suggestion is tested in the present work by comparing angle-resolved spectra from the silicon (111) 1×1 unreconstructed and (111) 7×7 reconstructed surfaces, respectively. Remarkable differences are observed in the two spectra, giving support to the suggestion that incoherent scattering of the outgoing beam is greatly enhanced by the reconstructed layer. The ability to produce two different structures on the one crystal surface was a factor in the choice of the silicon (111) surface for the present study, other factors being the well-documented method for preparing and cleaning this surface,¹⁷ plus the fact that the silicon band-structure is relatively well known.¹⁸

The present investigation has goals in addition to the above. In the extensive literature of SEE many models and theories have been put forward to describe processes that contribute to the secondary emission. Some of these theories attempted to account for specific steps in the overall SEE process on a microscopic basis. In most

cases the aim of calculations incorporating these theories was to account for the secondary yield, $\int_0^{2\pi} d\Omega \int_0^{E_{\max}} j_s(E, \Omega) dE$, and the secondary-energy spectrum, $\int_0^{2\pi} j_s(E, \Omega) d\Omega$. However, because there are many undetermined factors in these calculations the yield or spectral measurements themselves are not a good test of any individual feature of the calculations. One of the goals of this work, as of most of the previous EADSEE studies, is to investigate whether detailed EADSEE measurements provide a good test of the microscopic models and theories which exist. The question boils down to this: Are there regions of the spectra where structure is dominated just by one process? Only in these cases will it be possible to identify and study the processes important in SEE.

The experimental data is presented in Sec. II. In Sec. III theories and models for the three steps of secondary emission are described, attention being given to the range of energy over which each theory is applicable. The experimental data is discussed in terms of the models in Sec. IV. Many of the processes that contribute to structure in EADSEE are identified and studied.

II. RESULTS AND DISCUSSION

The EADSEE reported here for the $\langle 2\bar{1}\bar{1} \rangle$ and $\langle 10\bar{1} \rangle$ azimuths (Fig. 1) were recorded using the apparatus described previously, with energy and angular resolutions of 0.15 eV and 1.5° , respectively.^{13,19} In these experiments the electron-optic axis of both the monochromator and analyzer are co-planar with the surface normal of the crystal. Unless otherwise stated, the incident beam

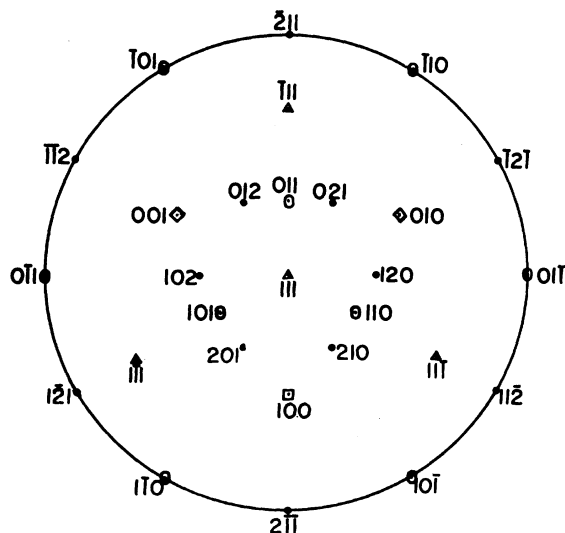


FIG. 1. Cubic (111) standard projection.

entered the crystal with a polar angle between 17° and 30° , in the azimuth opposite that of the analyzed secondaries.

The (111) 7×7 surface was thermally etched to an extent that pits and "lemon peel" structure were visible to the unaided eye. However, a clearly defined 7×7 ELED pattern was obtained from the surface for incident beam energies of 10–300 eV. It has been emphasized that an ELED pattern is not a sensitive indicator of surface perfection.²⁰ Random structural features in a surface cannot produce any diffraction effects aside from a decrease of beam intensities and a corresponding increase in the background intensity.²⁰ The well-defined ELED patterns, as well as the angular-dependent EADSEE structure observed for this surface, indicate that the condition of the surface in this experiment did not obliterate diffraction information.

The data for electrons emerging into the $\langle 11\bar{2} \rangle$ azimuth of the 7×7 surface, prepared as above, and for the $\langle 2\bar{1}\bar{1} \rangle$ azimuth of the 1×1 surface, prepared as described previously,¹³ were taken with a precursor instrument which had lower resolution, 0.5 eV. These earlier spectra were documented sufficiently for present purposes, although not to the extent of the more-recently-recorded data. In each case typical spectra are reported, the structure being reproducible. Only a selection of the spectra, which were recorded at least every 2° , are reported here.

The spectrum in Fig. 2(a) is for electrons emerging at 20° in the $\langle 2\bar{1}\bar{1} \rangle$ azimuth of a silicon (111) 1×1 surface. This particular spectrum was excited by a nominal 40-eV beam incident at 20° in the $\langle 211 \rangle$ azimuth. At the same angle of emergence the position of the peak at 32 eV in the secondary spectrum was insensitive to changes of incident beam condition of up to $+10$ eV, $\pm 5^\circ$. It cannot be an energy-loss peak. The peak at 9 eV appeared at the same emergence angle for all input-beam energies that were tried, which ranged between 15 and 50 eV. Structure of the same nature as that displayed in Fig. 2(a) has been observed in previously reported angle-resolved secondary spectra from tungsten¹⁶ and is expected from Kane's model. The EADSEE spectra from the (111) 1×1 surface, of which the spectrum of Fig. 2(a) is a part, do depend on the emergence angle in a manner which will be investigated in future work.

The spectrum from the (111) 7×7 surface at the same angle of emergence, and for the same incident beam conditions as the spectrum in Fig. 2(a), is shown in Fig. 2(b). Apart from a very weak energy-loss feature at about 34 eV, the spectrum is structureless from the initial peak,

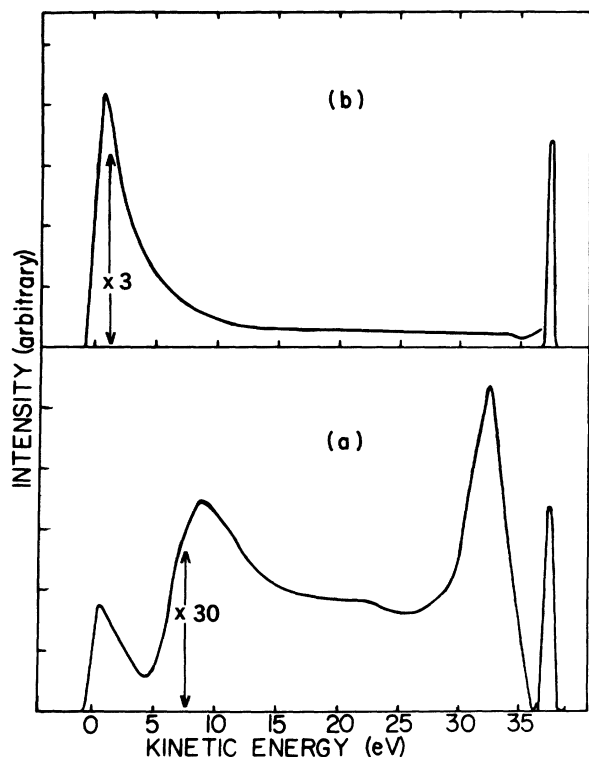


FIG. 2. (a) Secondary-electron emission spectrum emerging from a $(111) 1 \times 1$ surface in the $\langle 2\bar{1}\bar{1} \rangle$ azimuth, at a polar angle of $20^\circ \pm 1^\circ$. (b) Same, from a $(111) 7 \times 7$ surface.

at less than 0.50 V, to the elastic peak. There is no sign of the 9-eV or 32-eV peaks. The shape of the high-energy end of this spectrum, above 6 eV, did not change for the hundreds of different incident beam conditions that were tried, including incident energies from 30 to 300 eV and angles from 15° to 40° . The lack of structure between about 6 and 50 eV is typical of this energy region for spectra observed in all azimuths of the reconstructed surface which were studied here, for all input beam conditions tried.

When plotted as $j_s(E_0, \theta)$ curves, the data from the reconstructed surface display cosine behavior for $6 < E_0 < 50$ eV. Thus here, as well as in the study by Koshikawa *et al.*,¹² structureless $j_s(E, \Omega_0)$ curves accompany cosine behavior of $j_s(E_0, \theta)$ plots.

It is believed that the structure observed for the unreconstructed surface, and the cosine behavior observed for the reconstructed surface (Fig. 2), are further examples of the two types of spectra observed in previous EADSEE studies. The differences between the spectra in the present case can be attributed only to the surface.

An array of low-energy secondary spectra for

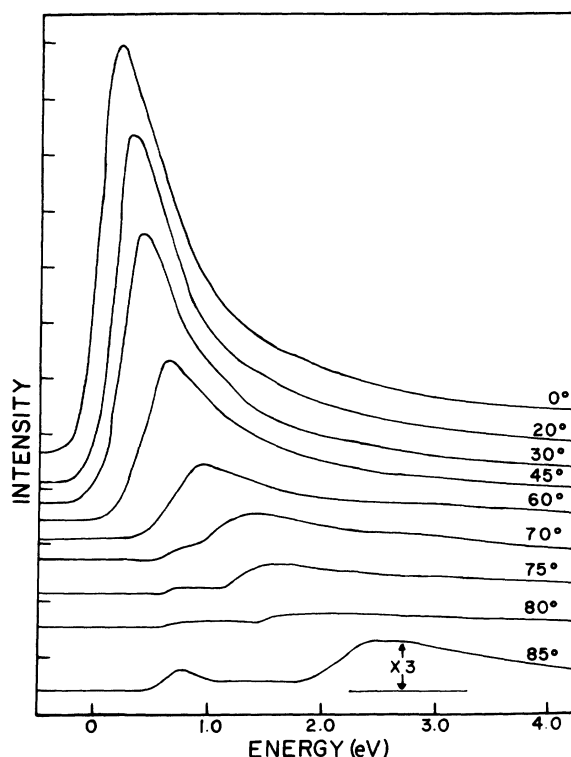


FIG. 3. EADSEE spectra for secondaries emerging into the $\langle 2\bar{1}\bar{1} \rangle$ azimuth of a $(111) 7 \times 7$ surface. The angle is between the direction of the emerging beam and the surface normal.

electrons emerging in the $\langle 2\bar{1}\bar{1} \rangle$ and $\langle 10\bar{1} \rangle$ azimuths, corrected for the entrance lens aberration,¹⁹ are shown in Figs. 3 and 4, respectively. These spectra were excited by a 50-eV incident beam. Angles are measured from the surface normal. The inflection point of the threshold of the spectrum of electrons emerging at 0° is taken as the zero of kinetic energy in the vacuum. Data for the $\langle 11\bar{2} \rangle$ azimuths are shown in Fig. 5.

For energies of less than about 6 eV there are differences in the spectra from the various azimuths. One qualitative similarity, however, is that the spectral thresholds move to higher energies as the angles of emergence increase. Apart from this threshold effect, the low-energy region of the $j_s(E, \Omega_0)$ curves for emission into the $\langle 2\bar{1}\bar{1} \rangle$ azimuth are featureless, the $j_s(E_0, \theta)$ curves exhibiting cosine behavior down to about 2.5 eV. A greater variety of structure is observed for emission into the $\langle 10\bar{1} \rangle$ and $\langle 11\bar{2} \rangle$ azimuths (Figs. 4 and 5); cosine behavior is not observed in this low-energy region.

One other type of measurement was made in this work. Spectra were measured at normal emergence for two different input-beam conditions. In

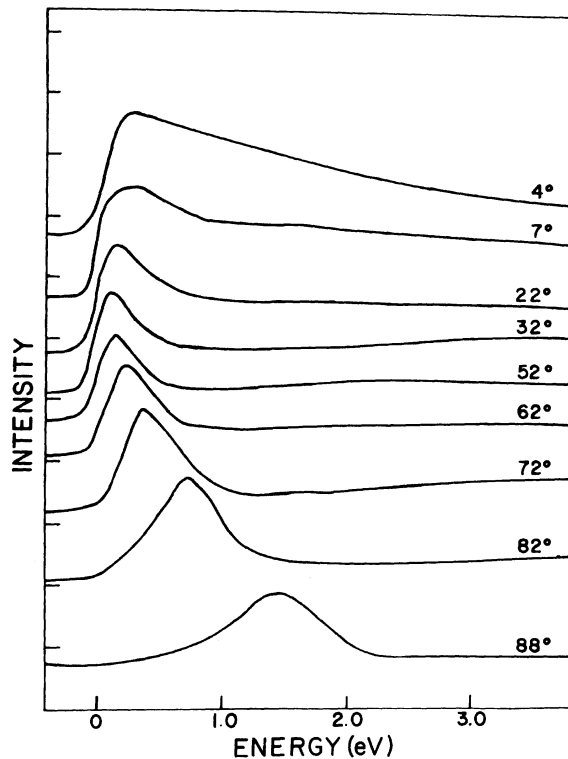


FIG. 4. EADSEE spectra for secondaries emerging into the $\langle 10\bar{1} \rangle$ azimuth of a $(111) 7 \times 7$ surface.

this case any observed differences must be associated with the excitation or transport steps and not the emergence step for which conditions are constant. Such comparisons have been made previously for secondary spectra without angular resolution.²¹ In Fig. 6 are spectra taken at normal emergence from the 7×7 surface, for two different values of incident electron energy, 32 and 320 eV, respectively. The ratio of the secondary current excited by a 320-eV incident beam to that excited by a 32-eV beam is plotted as a function of energy in Fig. 7. The ratio has been normalized to a value of 1 at 7 eV; it stays at 1 for energies down to about 3 eV and then rises rapidly, reaching a value of 3 by 0.125 eV, the lowest energy for which the ratio could be measured accurately.

This last measurement is of a somewhat different nature than the previous ones. However, it bears on the general question investigated here; the utilization of EADSEE measurements to gain understanding about specific processes important in SEE.

III. MODELS

A. Excitation

The steps that can lead to structure in EADSEE are listed in Table I. First, electrons must be

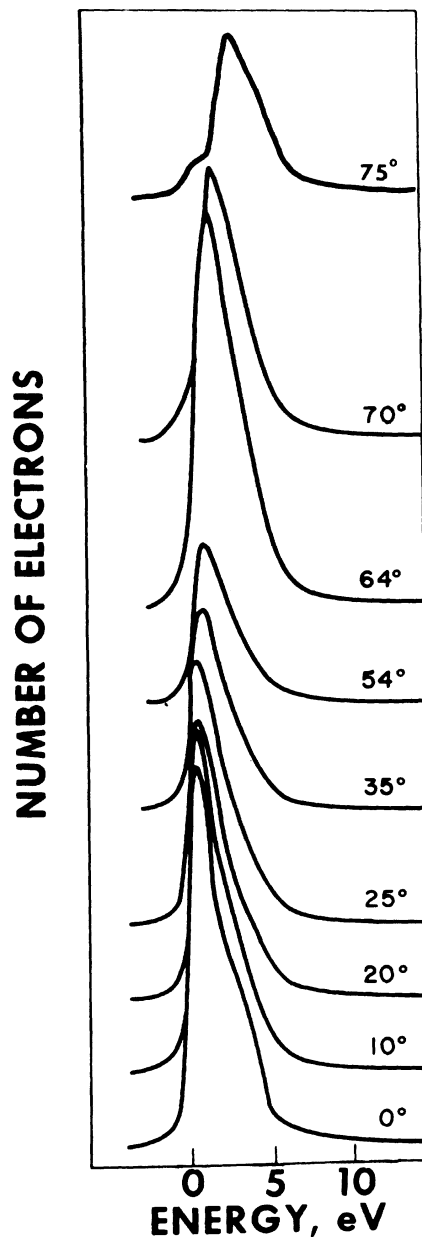


FIG. 5. EADSEE spectra for secondaries emerging into the $\langle 11\bar{2} \rangle$ azimuth of $(111) 7 \times 7$ surface.

excited from the valence band into high-lying conduction states. There are three ways this can happen; by direct excitation by the screened Coulomb field of the primary electron or another electron of sufficient energy, by excitation during the decay of a hole state by the Auger process, or by excitation due to plasmon decay.

The direct excitation by hot electrons was considered by Kane.¹⁴ For silicon he calculated directly the distribution of excited electrons in different bands, for the case of a low-energy ex-

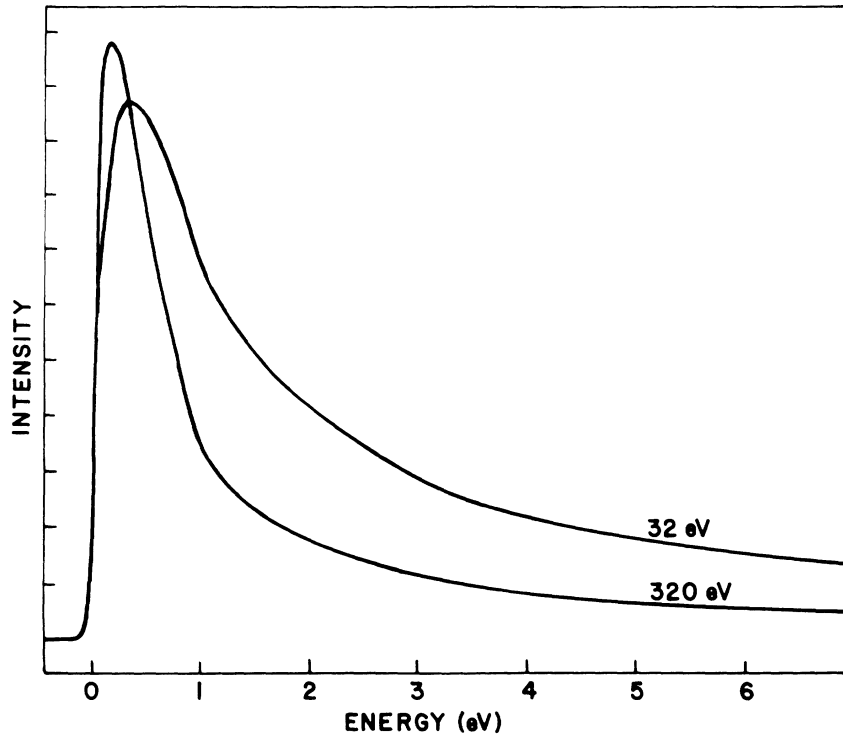


FIG. 6. Secondary spectra at normal emergence for 32- and 320-eV incident beam energies, respectively.

citing beam which lost energy primarily by pair production. Kane took into account energy and momentum conservation as well as considering the matrix element for Coulomb excitation. The results of these calculations agreed well with those derived from a "random- k " approximation in which momentum conservation was effectively ignored.¹⁴ In both cases structure in the hot-electron distribution mainly reflected structure in the density of conduction states, the final states of the excitation. In conjunction with the assumption of energy conservation for the electrons crossing into the vacuum, Kane's result has received support from a number of experiments. The most extensive work relating to this problem was the study of fine structure in the secondary-energy spectrum from graphite.¹⁵ Observed structure correlated well with structure in the density of conduction states in graphite. Angle-resolved spectra of electrons emerging normally from different faces of tungsten single crystals, measured by Willis, also gives strong support for this model.¹⁶ For the (100), (111), and (110) faces of tungsten the structure in the energy spectrum displayed the one-dimensional density of those states having $k_{\parallel} = 0$, where k_{\parallel} is the component of wave vector parallel to the surface.¹⁶

The highest electron energy considered in Kane's calculation was 8 eV above the top of the valence band. The model has been applied successfully

for much higher energies, however. The experimental work of Willis and others has shown that density-of-states structure is evident in secondary emission spectra up to 40 eV above the Fermi level.^{15,16} From these experimental and theoretical considerations it is expected that density-of-states structure will be present in the energy distribution of the electrons incident on the surface from within the silicon, over the energy range of interest in this work, < 40 eV.

Electrons arising from the Auger decay of silicon core hole states do not have energies in the region of interest of this paper.²² Electron-hole pairs can be produced by the Auger decay of deep valence holes. The density of conduction states is expected to be prominent in the energy spectrum of electrons produced in this way, as for the case of excitation by hot electrons.^{14,15}

For free-electron metals the decay of plasmons is mostly by processes other than electron-hole formation.²³ This is not the case for silicon in which single-particle excitations can occur over the whole energy region in which plasmons are formed. Decay by electron-hole pair formation is one reason for the large breadth of the plasmon loss peak in silicon, FWHM \approx 7 eV.²⁴ It seems unlikely that the decay of plasmons could produce structure in the hot-electron distribution which is narrower than this. It is therefore unlikely that the hot-electron distribution formed by plasmon decay

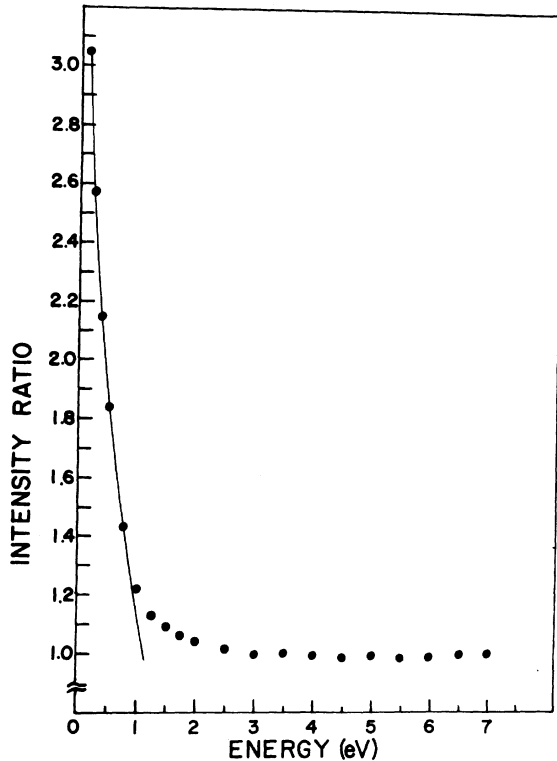


FIG. 7. Ratio of the intensity of the SEE current excited by a 320-eV primary beam to that excited by a 32-eV beam vs energy, normalized to a value of 1.0 at 7 eV. The dots are experimental points. The line is the result of the model calculation described in the text.

can account for any of the structure discussed in this paper. In short, the only significant structure in the "as-excited" hot-electron distribution, independent of input-beam conditions, is expected to reflect the density-of-states structure in the conduction band.

B. Transport

The energy distribution of the electron flux will be changed by inelastic scattering during the transport process. A complete discussion of this effect involves the consideration of scattering into and out of high-energy conduction-band states and has been the subject of a number of discussions based on transport theory.^{25,26} In the energy range below about 20 eV the effect of this scattering is to reduce the number of high-energy electrons relative to the number of low-energy electrons,²⁵ owing to the change of mean free path with energy.^{14,27} The greater the distance from the surface that the hot-electron flux is formed, the greater the relative depletion of the high-energy end of the flux when it reaches the surface. With increase in energy of the incident beam electron-

TABLE I. Steps that occur in the process of secondary emission.

Excitation	<ul style="list-style-type: none"> { By hot electrons By Auger decay of holes By plasmon decay
Transport	Inelastic scattering
Emergence	<ul style="list-style-type: none"> Elastic { Diffraction Refraction Transmission Inelastic

hole pairs will be excited at increasing distances from the surface. In this case, Bennett and Roth predicted the type of effect reported in Fig. 6.²⁵ This will be discussed in more detail below. It is clear that structure in the form of peaks is not introduced into the energy distribution by these transport effects.

Very small amplitude structure, actually a change of slope, has been detected in the secondary-electron spectrum from silicon at one-plasmon energy above the bottom of the conduction band.²³ Electrons with energy greater than this can be removed from the outgoing flux by creating plasmons. The structure, detected by a derivative technique, is sufficiently small to escape detection in the present work.²³

Also affecting the shape of the hot-electron distribution is the velocity dependence of the mean free path. As discussed by Kane and others,^{6,14} the probability for scattering of an electron is inversely proportional to its group velocity. Electrons are therefore scattered most rapidly out of states of high density. This velocity-dependent scattering would tend to smooth out the original spectral structure caused by the excitation process. There is no evidence that this process is important in the present results.

C. Emergence

To this point of our consideration the significant structure in the electron-energy distribution originates in the excitation process and reflects structure in the conduction-band density of states. When the outgoing electrons impinge on the surface they can be reflected back into the solid, they can emerge elastically into the vacuum, or they can be scattered inelastically. The back reflection will manifest itself as a transmission coefficient, for emergence, of less than unity. Structure that can be introduced into EADSEE by these processes will be considered. At this time it is not possible to predict the relative probability with which these

competing processes occur; that can be found only from a comparison between observed structure and that predicted by the model for each process.

1. Elastic emergence

a. Diffraction and nonunity transmission. The case of elastic emergence, which has been treated widely in ELEED, will be considered first. An electron coherently crossing a two-dimensional barrier will have

$$k_{\parallel \text{ out}} = k_{\parallel \text{ in}} + b_{\parallel} \quad (1)$$

where k_{\parallel} is the component of the electron wave vector parallel to the surface, and b_{\parallel} is a surface reciprocal lattice vector.²⁸ The occurrence of nonzero values of b_{\parallel} in this process can be considered equivalently as diffraction by the two-dimensional lattice of surface atoms. This diffraction can occur over most of the energy range of interest in the present work. This process can cause a maximum in the internal electron spectrum to be distributed into a number of angles of emergence.

In one theory of ELEED the intensity of each diffracted beam can be predicted by matching the amplitudes and their normal spatial derivatives of the internal and external waves, respectively, at the boundary, taking into account the presence of surface-state resonances with the same value of k_{\parallel} .²⁹ The same formalism has been used to calculate transmission coefficients for the case of electrons with energies just above threshold, in studies relating to field and thermionic emission.^{30,31} These latter calculations, which have been performed on metals without reconstructed surfaces, indicate that the transmission coefficient is close to unity down to very small values of k_{\perp} , 0.2 (eV).^{1/2} Reflection of the outgoing beam could cause attenuation of the lowest-energy regions of the $j_s(E, \Omega_0)$ spectra. A barrier more complicated than a step will change this result quantitatively but not qualitatively.

Experimental results have been interpreted in a way that suggests that transmission coefficients of magnitude considerably less than unity occur for relatively high-energy (~ 50 eV) electrons impinging on a reconstructed surface.³² It is not known if this process can lead to structure in EADSEE.

b. Refraction. Refraction is the third emergence phenomenon that can affect the shape of EADSEE spectra. This effect has been discussed by a number of authors, all on a free-electron model.^{4,5,25} Making use of the equation of continuity at the surface and of the law of refraction, Bennett and Roth showed that²⁵

$$\frac{j_s(E, \theta)}{j_s(E, 0)} = \frac{T(E', \theta')N(E', \theta') \cos \theta}{T(E', 0)N(E', 0)} \quad (2)$$

where the primes refer to quantities inside the solid, T is the transmission coefficient, and $N(E', \theta')$ is the distribution of electrons just within the surface, the result of excitation and transport processes. The quantity of the left-hand side of Eq. (2) is a prediction of the normalized polar plot of EADSEE. As $E \rightarrow 0$, $j_s(0, \theta)/j_s(0, 0) = \cos \theta$, predicting cosine behavior of the polar plot.²⁵ At higher energies, prediction of the polar behavior of $j_s(E_0, \Omega)$ by (2) requires knowledge of $T(E', \theta')$ and $N(E', \theta')$, which is generally not available. No prominent EADSEE structure is expected to be caused by refraction. The results of this analysis are not affected by the presence of a complicated potential barrier at the surface.

2. Emergence with inelastic scattering

Other than reflection or coherent emergence, an electron can be inelastically scattered as it traverses a reconstructed surface layer. This process has not been considered previously in discussions of secondary emission. In conjunction with the previous EADSEE results, the data of Fig. 2 make it necessary to consider this possibility. The behavior expected for $j_s(E_0, \Omega)$ will be considered for this case in an attempt to account for both the obliteration of the structure in EADSEE and the cosine behavior observed for $j_s(E_0, \theta)$ from the reconstructed surface.

If the incoherent scattering of the outgoing beam were predominantly in the forward direction, residual structure would still be observed in EADSEE. Such would be the case for emerging energies above 200 eV. For the energies of interest in this paper, < 40 eV, plasmon excitation occurs with small probability,³³ and the scattering that accompanies single-particle excitations can occur with high probability over an appreciable range of angles.³⁴ The electron states in the vacuum will be occupied according to their local density in this type of scattering,^{14,34} The spatial distribution of the density of vacuum states is isotropic, therefore the number of electrons per unit solid angle, emitted from each point of the surface, is isotropic. For a detector viewing an area larger than the irradiated area,¹⁹ the number of electrons received will then depend on the surface area seen by the detector. That is, the intensity will depend on the projection of the irradiated area onto the normal to the line of sight, which is proportional to $\cos \theta$ (Fig. 8). It is proposed that incoherent scattering by the surface layer gives rise to cosine behavior of $j_s(E_0, \theta)$ in this manner. To establish this model quantitatively

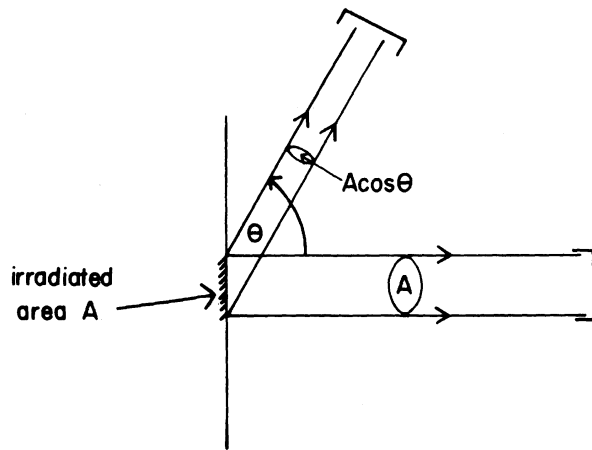


FIG. 8. An area A of the surface is irradiated by the incident electron beam. At a take-off angle of θ relative to the surface normal a detector sees a surface area of $A \cos \theta$.

one would need to consider the spatial characteristics of the internal electron flux, diffraction-assisted incoherent scattering, and details of the Coulomb scattering itself.

As for the case of scattering within the solid,^{6,14} it is possible that the probability for inelastic scattering on emergence depends on the internal velocity of the electron. This process could also reduce the amplitude of structure observed in the spectra of electrons emerging from the reconstructed surface.

It is recalled that while EADSEE in the $\langle 2\bar{1}\bar{1} \rangle$, $\langle 10\bar{1} \rangle$, and $\langle 11\bar{2} \rangle$ azimuths are essentially the same in the energy region above about 6 eV; they differ for energies lower than this. Without introducing additional assumptions the incoherent scattering model cannot explain this observed difference and, therefore, cannot be used to describe the low-energy end of the spectra. There are several reasons why this scattering does not occur for the low-energy electrons.

The mean free paths of electrons in solids increase as the electron energies approach the Fermi energy from several eV above it.²⁷ With reduced electron energy, the number of possible final states for pair production becomes less, so the probability for scattering becomes less.¹⁴ More particularly, at this silicon surface which has an ionization potential of 5 eV,³⁵ scattering events in which both final states are vacuum states only become possible for initial states with energies 5 eV above the vacuum level. Most of the electrons incident on the surface with energies less than 5 eV will probably escape into the vacuum without inelastic scattering or will be reflected back into the solid. In addition, incoherent scat-

tering of high-energy emerging electrons will occupy vacuum states according to their local density which goes as $E^{1/2}$.^{14,34} Inelastic scattering is not a plentiful source of very-low-energy secondaries. Overall, then, it is expected that at and near threshold all the observed electrons emerge coherently from bulk states; none are from incoherent surface scattering events. The relative number of detected electrons which have been incoherently scattered into vacuum states will increase with increase in energy. In general, inelastic scattering of the emerging flux removes peak structure from the EADSEE spectra.

IV. DISCUSSION

A. Spectra above 6 eV

The EADSEE data will be discussed with the models described in Sec. III. The structure reported in the energy region above 6 eV in Fig. 2(a), for the unreconstructed surface, must reflect structure in the energy distribution of electrons inside the silicon. No other source of high-energy structure has been hypothesized. The observation of this structure implies that electrons in the appropriate bulk states emerge through the unreconstructed surface without appreciable inelastic scattering. The lack of similar structure in the data for the reconstructed surface, Fig. 2(b), as well as the cosine behavior of $j_s(E_0, \theta)$, is taken as evidence that few of the electrons in this energy range emerge elastically through the reconstructed surface. In this case the observed spectra are the result of incoherent scattering of the outgoing electron flux. The observation implies a very short mean free path for electrons in the reconstructed layer, shorter than "normal" for electrons in this energy range.²⁷ To understand such short mean free paths, it is noted that a reconstructed surface could well have an electronic band structure which does not match that of the bulk at all. Before passing into the vacuum, electrons in bulk states would need to pass through a forbidden energy region in the surface electronic structure. Mean free paths of electrons in such forbidden regions can be sufficiently short, $< 3 \text{ \AA}$, to explain the large probability for incoherent scattering of the emergent beam.⁶ Because of the large scattering it is probable that the bulk crystal structure of silicon will be probed very little by ELEED investigations of this surface, in this energy range.

B. Spectra below 6 eV

1. Bulk band structure

Below 6 eV the spectra for different azimuthal angles of emergence are quite different. For this

and the reasons mentioned in Sec. III, it is probable that the electrons observed in this low-energy region have emerged coherently across the reconstructed surface. The most prominent structure is observed for the $\langle 11\bar{2} \rangle$ azimuth. The threshold of the spectra moves to higher kinetic energies as the angle from the normal increases, until a prominent peak appears at an energy of 0.9 eV for angles from 30° to 64° , and then moves to 1.4 eV at 72° , where it remains for 2° , thereafter appearing at higher energies for increasing angles of emergence (Fig. 5). This will be discussed in terms of Kane's model for the excitation process, in conjunction with energy and k_{\parallel} conservation for the emergence process.

Because of k_{\parallel} conservation, electrons observed in one plane of emergence originate from crystal states having wave vectors that lie in the same plane. For a face-centered-cubic crystal, electrons emerging in the $\langle 11\bar{2} \rangle$ azimuth originate from the plane of k space defined by the points ΓLK (Fig. 9). To compare theory with experiment, one would note that

$$\theta = \sin^{-1} \{ \hbar k_{\parallel} / [2m(E - E_{\text{vac}})]^{1/2} \} \quad (3)$$

is a constant for all states contributing to the energy spectrum recorded at an angle of emergence θ , where E_{vac} is the vacuum level. This is a prescription for selecting those states, from a band-structure calculation, which contribute intensity to secondary emission into the polar angle θ . In (3), k_{\parallel} and E would be calculated for each state, from the band-structure results. The density of states at each value of energy would then be summed for all of these states to produce a spectrum. Structure in the resulting plot of intensity versus en-

ergy should bear a close resemblance to structure in the appropriate $j_s(E, \Omega_0)$ curve. In this discussion the possible contribution of nonzero values of b_{\parallel} , Eq. (1), has been neglected.

Band-structure results have been published for the symmetry directions ΓL and ΓK and for the zone boundary LK , but not for the complete ΓKL plane that can contribute to SEE in this azimuth.¹⁸ Because of this the model described above cannot be utilized, and an approximate method for comparing theory and experiment will be described. Symmetry arguments can be used to show that state densities will have local maxima along symmetry directions or across zone boundaries. It is then assumed that peaks in the secondary spectra are due to electrons which emerge from bulk state having k vectors along the symmetry directions, or terminating on a zone boundary, in the plane of k space which includes ΓLK . The observed $E-\theta$ data can thus be transposed to $E-k$ data for these principal directions. The method is not unambiguous at this stage as there is more than one possible principal direction in the k plane that could contribute spectral maxima in one plane of emergence. The ambiguity is removed by comparing the $E-k$ curves deduced from experiment with those derived from the available band-structure calculations. This has been done for the peaks in Fig. 5. The $E-\theta$ values for each peak have been converted to $E-k$ information for the Λ , Σ , and $L-K$ directions. Using the ionizational potential of this surface, 5.0 eV,³⁵ the experimental and theoretical curves can be compared. This is done in Fig. 10 for the Σ direction. Excellent agreement is observed; certainly within the estimated error bounds of the experimental data, ± 0.4 eV. The results are self-consistent in that peaks are ob-

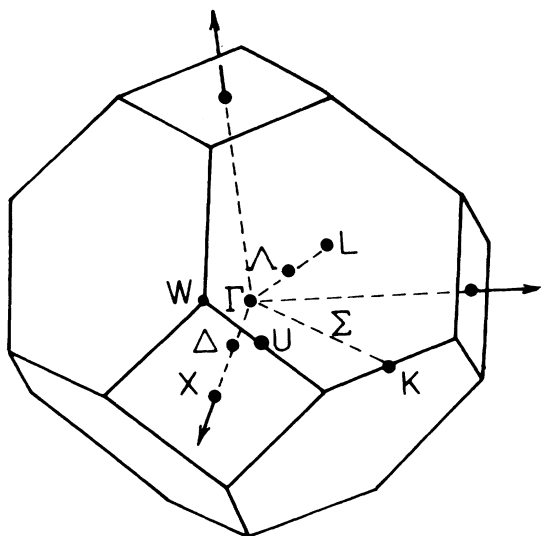


FIG. 9. The first Brillouin zone for the fcc lattice.

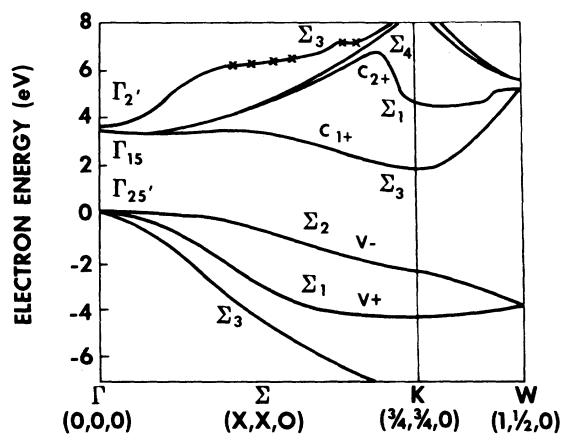


FIG. 10. Band structure of silicon along the Σ direction, as calculated by Kane (Ref. 18). The data points were deduced from the spectra reported in part in Fig. 5, in a manner described in the text.

served for electrons emerging from regions of very high state density.³⁶

Peaked structure is not observed for the EADSEE spectra recorded for the $\langle 2\bar{1}\bar{1} \rangle$ azimuth. This observation is consistent with the model, as large density-of-states variations do not occur in the symmetry directions involved.¹⁸ The poorly defined structure in the $\langle 10\bar{1} \rangle$ azimuth (Fig. 4) occurs at energies and angles at which possible structure from density-of-states effects overlaps with that from transmission effects. Consistent with the aims of this paper, an interpretation of this overlapping structure will not be attempted.

2. Refraction

Three features can be observed in the spectra of electrons emerging into the $\langle 2\bar{1}\bar{1} \rangle$ azimuth (Fig. 3). For energies above 2.5 eV there is cosine behavior of $j_s(E_0, \theta)$. It is believed that this behavior is due to refraction, as discussed immediately below. There is a marked reduction of intensity below that of cosine behavior for the lowest energies observed for angles of emergence of 20° – 85° (Fig. 3), and there is a footlike structure at 0.8 eV at angles of 70° – 85° . These features are discussed in terms of transmission and diffraction, respectively.

The simplest way to interpret the cosine behavior is to postulate an $N(E', \theta')$ which is constant with θ' in this energy range, a value of $T(E', \theta')$ which is equal to unity, and to ascribe the cosine behavior to the refraction effect [Eq. (2)]. This description implies that the dispersion curves in this energy and k -vector region are free-electron-like; more specifically, that the curves are free-electron-like in a region of k space extending from the Λ direction to a direction about 20° from Λ toward Δ (Fig. 9), within 2.5 eV of the vacuum level. Theoretical band-structure results for the region of k space have not been published.

3. Threshold behavior

The lack of low-energy electrons emerging into the $\langle 2\bar{1}\bar{1} \rangle$ azimuth with polar angles between 30° and 85° , Fig. 3, will be considered here. It was first suspected that residual magnetic or electric fields, or perhaps electric fields associated with surface defects, were responsible for deflecting the lowest-energy electrons from the desired straight-line paths. If this were the case their lack of detection could cause the observed low intensities. However, from these same surfaces emission from surface-state resonances is observed at energies below the "cutoff" energies reported in Fig. 2 for angles greater than 60° .¹³ The lack cannot readily be explained as an experimental artifact.

The results of band-structure calculations are available for the Σ -, Δ -, and Λ -symmetry directions.¹⁸ From these curves it would appear that there are states in the region of energy and wave-vector space corresponding to the energies and angles for which deficiencies are observed, i.e., there is probably not an energy gap. It should be possible for electrons to be excited into such states and to travel to the surface. The lack of low-energy electrons is attributed to the emergence stage of secondary emission. As mentioned in Sec. III, calculations of transmission coefficients for emergence are not available for semiconductors. One factor to enter into such calculations will now be described. For transmission across a surface whose normal is a two, four, or six fold rotation axis for the bulk, reflection back into the crystal can take place into states which mirror those of the incoming beam. In this case the calculation of the transmission coefficient for oblique incidence is similar to that for normal incidence. For transmission across surfaces of different symmetries there will in general be fewer bulk states for the electron to be reflected into.³⁷ Therefore, electrons incident on the surface more obliquely would emerge into the vacuum with greater probability.

In what follows the EADSEE data will be analyzed from the point of view of threshold transmission. This is partly to show the effect of the lack of reflection symmetry on the transmission coefficient for SEE from this surface, and partly to introduce this type of measurement in order to illustrate its potential utility.

The data will be treated as if it were measured for a one-dimensional system. In that case, the probability for an incident electron to be transmitted across the boundary is commonly plotted against k_\perp . The transmission coefficient is the fraction of the incident electrons that emerge into the vacuum, after correcting for refraction effects. The approximation adapted here makes use of the free-electron-like character of the band structure for electrons emerging in the $\langle 2\bar{1}\bar{1} \rangle$ azimuth just above threshold, discussed in the last paragraph Sec. IV B 2. As described above, for an assumed transmission probability of one, the intensity falls as the cosine of the angle between the direction of emergence and the surface normal, due to refraction. Intensity reduction beyond that predicted for cosine behavior is attributed to the transmission coefficient. With these assumptions the curves of transmission vs k_\perp were calculated and are shown in Fig. 11. In many of the curves there is a foot structure. This structure is discussed later.

The value of k_\perp associated with the inflection

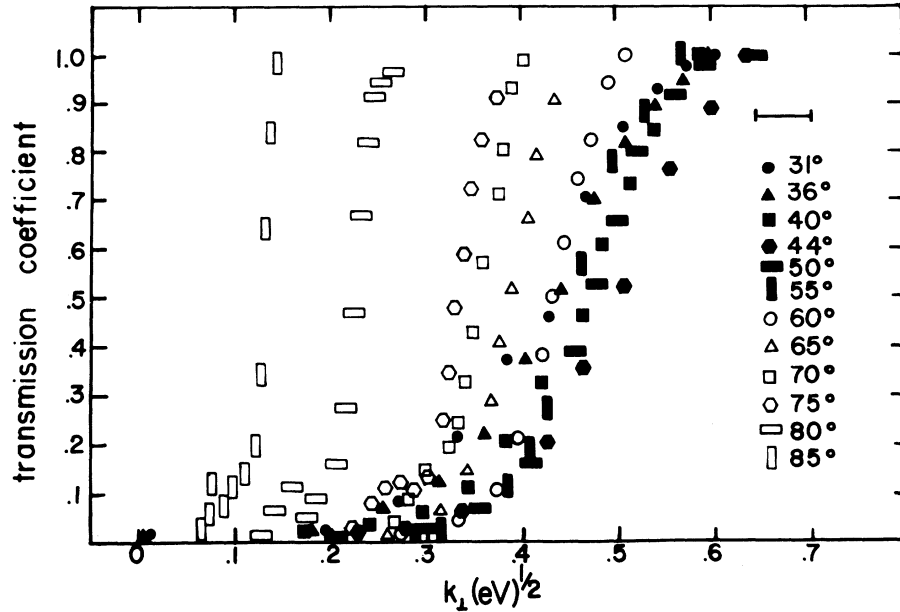


FIG. 11. Transmission coefficient vs the component of external wave vector normal to the surface for electrons incident on the (111) 7×7 surface in the $\langle 2\bar{1}\bar{1} \rangle$ azimuth.

point of the main threshold is at 0.50 ± 0.05 (eV) $^{1/2}$ for angles of emergence from 36° to 55° (Fig. 11). The inflection point then moves to much smaller values of k_\perp , reaching 0.13 (eV) $^{1/2}$ for emergence at 85° . As the electrons incident on the (111) surface from within make larger angles with the surface normal their chance of having a state to be coherently reflected into within the solid is reduced; the probability for them to emerge into the vacuum increases. This effect could cause the observed movement of the inflection point with increase in angle of emergence.

The determination of transmission coefficients by this method requires justification beyond that provided here. The method described here could follow the inflection point of a transmission curve to values of E_\perp of less than 0.005 eV. This would represent an improvement over measurements obtained by existing techniques.^{30,31}

4. Diffraction of secondaries

For angles of emergence from 60° to at least 85° in the $\langle 2\bar{1}\bar{1} \rangle$ azimuth (Fig. 3) there is a foot structure just prior to the onset of the main emission. The peak of the structure is at 0.80 ± 0.2 eV for all angles of emergence for which it is observed. The values of energy and angle measured for this series of peaks do not match those measured for structure believed due to emission from surface states.¹³ It is unlikely that the structure is due to the transmission factor for any potential barrier consisting of one or two

steps.³⁸

The peak structure is probably due to structure in the bulk density of states. First to be considered in this case is emission from states in the half-plane of k space ΓLX . Such emission could occur with $b_\parallel = 0$ [Eq. (1)] to contribute to the foot structure. However, there are no maxima in the density of states along high-symmetry directions, at the appropriate energy region, in ΓLX .¹⁸ For the case of emergence into the vacuum with $b_\parallel \neq 0$, there are regions of k space with density-of-states maxima at the appropriate energy. These are the same states which gave rise to structure in the $\langle 11\bar{2} \rangle$ azimuth, Fig. 5. Electrons emerging into the vacuum from these states with

$$k_{\parallel \text{ out}} = k_{\parallel \text{ in}} + 2b_\parallel,$$

where b_\parallel is 0.53 (eV) $^{1/2}$, would be detected at take-off angles from 60° to 90° in the $\langle 2\bar{1}\bar{1} \rangle$ azimuth. In the present case their clear observation depends on the lack of emission from other sources, and so they are observed only for angles of 60° – 85° . The agreement between the observations made in the $\langle 11\bar{2} \rangle$ and $\langle 2\bar{1}\bar{1} \rangle$ azimuths, respectively, as well as with the calculated band structure, is within experimental error.

In the absence of unforeseen excitation effects, this evidence indirectly reflects on the question of transmission across the surface barrier also. With diffraction, electrons from states in the ΓK direction are able to emerge into the vacuum at energies and angles for which states in the ΓLX plane have very low probability of emergence.

5. Effect of transport

As described in Sec. II the differences between the spectra in Fig. 6 must be due to differences in excitation and/or energy-dependent transport losses. Single-particle excitations are the main cause of energy loss for electrons with energies of about 30 eV and less.^{33,34} For single-particle excitations, conduction states will be occupied primarily according to their local density. This density is a slowly varying function for states with \vec{k} in the Λ direction¹⁸ and cannot account for the variation with energy shown in Fig. 6.

For electrons with energies above about 50 eV the dominant energy-loss mode in silicon is that due to the excitation of plasmons.^{33,34} Electrons are subsequently excited into high-lying conduction states by the decay of the plasmons. Because the plasmon-loss peak is very broad (Sec. III) the Coulomb excitation of electrons by plasmon decay cannot account for the narrow structure shown in Fig. 7.

These arguments imply that the energy spectrum of electrons excited locally into high-lying conduction states does not vary significantly from point to point within the solid. The structure in the curve of Fig. 7 is due primarily to transport effects.

Before discussing further the secondary emission some information concerning mean free paths of electrons in silicon will be presented. Kane has calculated that the mean free path varies from about 380 to 25 Å for electrons with energies ranging from 0 to 3 eV above the vacuum level, respectively.¹⁴ For energies greater than 3 eV the variation of the mean free path with energy, for electrons in allowed bands, is relatively slower.¹⁴ Evidence for mean-free-path values of 10–20 Å can be found for electrons in the 30–300-eV range.²⁷ Estimates I have made of the depth to which incident 30-eV electrons could excite secondaries range from 30 to 100 Å, depending on assumptions made about the energy and the wave vector for an average single-particle excitation. More-definite statements can be made concerning the penetration of the 320-eV incident beam. This beam will excite plasmons to a depth of about 600 Å, depositing its energy fairly uniformly along the path.²⁷

The following conclusion can be drawn from the mean-free-path data. For the lowest energies of the measured secondary spectra at normal emergence, i.e., less than about 2 eV, all electrons excited into conduction states with appropriate wave vectors, by the 32-eV beam, will reach the

surface. The distribution of secondaries recorded for the 32-eV exciting beam is taken to represent the original excitation function multiplied by a transmission factor. For electrons excited by the 320-eV beam, only those within a couple of mean free paths from the surface will reach the surface with high probability. In this case the distribution of secondaries that come from a particular depth z is proportional to $N(E)e^{-z/\lambda(E)}$, where $N(E)$ is the excitation function, and λ is the mean free path, remembering the assumption that the 320-eV beam deposits its energy uniformly along its path. With these approximations the spectral ratio depicted in Fig. 7 becomes proportional to $[N(E)\int_0^{600\text{ Å}} e^{-z/\lambda(E)} dz]/N(E)$, which is equal to $\lambda(E)$ for the present cases where the 600 Å is considerably greater than $\lambda(E)$. Normalizing Kane's mean-free-path data to the ratio of Fig. 7 at 0.125 eV, and depicting the result (mean free path versus energy) by a line, it can be seen that the proportionality holds very well over an intensity ratio range of 3.05–1.3.

There are two possible reasons for the deviation from proportionality that sets in at about 1 eV. If the 32-eV beam does excite secondaries to a depth of about 100 Å the assumption that all conduction electrons excited by this beam can reach the surface begins to fail at an energy of about 1 eV. It was described above how most SEE observed above 6 eV arises as a result of incoherent scattering of high-energy electrons impinging on the surface from within. There could be contributions to the low-energy flux from this scattering. This extra source of low-energy secondaries could also lead to the deviation shown in Fig. 7. That such a simple model can apparently account for the significant structure in the curve of Fig. 7 is more remarkable than the deviation.

V. CONCLUSIONS

The two types of structure observed previously in EADSEE have been observed here and have been associated with specific microscopic steps in the secondary-emission process. The main conclusion of the work is that individual processes important in SEE can be identified and studied by EADSEE. Our understanding of all the processes identified in the present investigation would benefit from further experimental study. There are many aspects of the present results, particularly those concerned with the derivation of transmission coefficients, that would benefit from theoretical input.

*Supported by a grant from the NSF.

- ¹G. Appelt, Phys. Status Solidi 27, 657 (1968).
- ²P. E. Best (unpublished).
- ³L. Austin and H. Starke, Ann. Phys. (Leipz.) 9, 271 (1902).
- ⁴O. Hachenburg and W. Brauer, *Advances in Electronics and Electron Physics*, edited by L. Marton (Academic, New York, 1959), Vol. 11, p. 413.
- ⁵H. G. McKay, Adv. Electron. 1, 65 (1948); H. Bruining, *Physics and Applications of Secondary Electron Emission* (McGraw-Hill, New York, 1954); R. Kollath, Handb. Phys. 21, 232 (1956); A. J. Dekker, Solid State Phys. 6, 251 (1958).
- ⁶P. J. Feibelman and D. E. Eastman, Phys. Rev. B 10, 4932 (1974).
- ⁷H. L. H. Jonker, Philips Res. Rep. 12, 249 (1957).
- ⁸H. E. Farnsworth, R. E. Schlier, T. H. George, and R. M. Burger, J. Appl. Phys. 29, 1150 (1958).
- ⁹J. Burns, Phys. Rev. 119, 102 (1960).
- ¹⁰M. P. Seah, Phys. Status Solidi 31, K123 (1969).
- ¹¹M. P. Seah, Surf. Sci. 17, 132 (1969).
- ¹²T. Koshikawa, R. Shimizu, K. Goto, and K. Ishikawa, J. Phys. D 7, 462 (1974).
- ¹³P. E. Best, Phys. Rev. Lett. 34, 674 (1975).
- ¹⁴E. O. Kane, Phys. Rev. 159, 624 (1967).
- ¹⁵R. F. Willis, B. Fitton, and G. S. Painter, Phys. Rev. B 9, 1926 (1974).
- ¹⁶R. F. Willis, Phys. Rev. Lett. 34, 670 (1975).
- ¹⁷C. C. Chang, Surf. Sci. 23, 283 (1970).
- ¹⁸E. O. Kane, Phys. Rev. 146, 558 (1966).
- ¹⁹P. E. Best, Rev. Sci. Instrum. 46, 1517 (1975).
- ²⁰P. J. Estrup and E. G. McRae, Surf. Sci. 25, 1 (1971).
- ²¹A. R. Shul'man, Yu. A. Morozov, and V. V. Korablev, Fiz. Tverd. Tela 11, 1360 (1969) [Sov. Phys.-Solid State 11, 1101 (1969)].
- ²²T. W. Rusch, J. P. Bertino, and W. P. Ellis, Appl. Phys. Lett. 23, 359 (1973).
- ²³V. E. Henrich, Phys. Rev. 7, 3512 (1973).
- ²⁴H. R. Philipp and H. Ehrenreich, Phys. Rev. 129, 1550 (1963).
- ²⁵A. J. Bennett and L. M. Roth, Phys. Rev. B 5, 4309 (1972).
- ²⁶G. F. Amelio, Vac. Sci. Technol. 7, 593 (1970); G. F. Dionne, J. Appl. Phys. 44, 5361 (1973).
- ²⁷C. J. Powell, Surf. Sci. 44, 29 (1974), and references therein.
- ²⁸C. B. Duke and G. E. Laramore, Phys. Rev. 3, 3183 (1973), and references therein.
- ²⁹D. S. Boudreaux and V. Heine, Surf. Sci. 8, 426 (1967).
- ³⁰P. H. Cutler and J. C. Davis, Surf. Sci. 1, 194 (1964).
- ³¹J. W. Gadzuk and E. W. Plummer, Rev. Mod. Phys. 45, 487 (1973), and references therein.
- ³²B. Goldstein, Surf. Sci. 35, 227 (1973).
- ³³P. S. P. Wei and A. W. Smith, Surf. Sci. 27, 675 (1971); M. F. Chung and L. H. Jenkins, Surf. Sci. 26, 649 (1971).
- ³⁴E. Bauer, Z. Phys. 224, 19 (1969).
- ³⁵M. Erbudak and T. E. Fischer, Phys. Rev. Lett. 29, 732 (1972); J. E. Rowe and H. Ibach, Phys. Rev. Lett. 32, 421 (1974).
- ³⁶This discussion was reported in preliminary form by P. E. Best, Bull. Am. Phys. Soc. 14, 794 (1969).
- ³⁷Similar effects for electrons whose energies are below the vacuum level have been discussed by E. A. Stern, Phys. Rev. 162, 565 (1967).
- ³⁸P. E. Best (unpublished).